Ectopic Matrix Metalloproteinase 9 Expression in Human Brain Tumor Cells Enhances Oncolytic HSV Vector Infection

Chang-Sook Hong[1], **Wendy Fellows**[2], **Ajay Niranjan**[2], **Sean Alber**[3], **Simon Watkins**[3], **Justus B. Cohen**[1], **Joseph C. Glorioso**[1], and **Paola Grandi**[2,*]

[1]Department of Microbiology and Molecular Genetics, University of Pittsburgh School of Medicine, Pittsburgh, PA 15261

[2]Department of Neurological Surgery, University of Pittsburgh School of Medicine, Pittsburgh, PA 15261

[3]Department of Cell Biology and Physiology, University of Pittsburgh School of Medicine, Pittsburgh, PA 15261

Abstract

Oncolytic HSV (oHSV) vectors have shown promise in the treatment of patients with recurrent brain tumors although few complete responses have accrued. Impediments to effective therapy include limited vector distribution on delivery, a consequence of injected virion particle trapping in the tumor extracellular matrix (ECM). To enhance virus delivery and spread, we investigated the use of the matrix metalloproteinase 9 (MMP9) as a means to degrade collagen type IV, a major component of the ECM and basement membranes of gliomas that is absent in normal brain tissue. SK-N-AS neuroblastoma cells were transduced for constitutive, elevated expression of MMP9, which did not enhance tumor cell migration in vitro or tumor progression in a murine xenograft brain tumor model. MMP9 expression afforded increased distribution of oHSV vector-infected tumor cell spheroids and afforded vector infection over larger areas of brain tumors in vivo. These results suggest that vector delivery and distribution in vivo can be improved by compromising the ECM, potentially enhancing oncolytic efficacy.

Introduction

Early phase human clinical trials have demonstrated that oncolytic HSV vectors (oHSV) as a therapy for recurrent brain tumors are safe without treatment-related severe adverse events and with some evidence of efficacy (1). However, impediments remain for efficient tumor killing that relate, in part, to initial vector distribution and subsequent virus replication and spread within the tumor. In particular, the ECM, which is largely manufactured by the tumor cells, can trap injected virus particles and prevent their diffusion (2). Several reports describe improved oHSV vector spread and tumor mass reduction in flank tumor models of sarcomas and melanomas following co-injection with matrix metalloproteinases (MMPs) (2, 3). However, experiments evaluating the use of MMPs to enhance vector distribution in models of brain tumor, the principal intended targets of oHSV, have not been reported.

Gliomas produce an ECM rich in type IV collagen and vitronectin. MMP-9 specifically targets type IV collagen and is therefore an attractive candidate for modifying the ECM to potentially increase oncolytic virus mobility and thereby infection range. To evaluate the

[*]Corresponding Author: Paola Grandi, PhD Assistant Professor of Neurological Surgery University of Pittsburgh School of Medicine Pittsburgh, PA 15261 PAG24@pitt.edu.

effect of MMP-9 expression on vector distribution, we employed a new oHSV vector designated JD0G in which eGFP replaced ICP0 expression and the joint elements separating the unique long and short components of the viral genome were deleted. Here we show that ectopic MMP-9 expression in neuroblastoma cells (i) does not increase tumor cell migration in vitro or enhance tumor growth in the brain, and (ii) increases the efficiency of infection by JD0G of tumor spheroids in vitro and promotes JD0G vector distribution throughout the intracranial tumor mass.

Materials and Methods

Cell lines and virus

Human glioblastoma SNB19, U251, and U373 (kindly provided by Dr. H. Okada, University of Pittsburgh), neuroblastoma SK-N-AS (ATCC, Manassas, VA), and osteosarcoma U2OS (ATCC) cell lines were cultured by standard methods. The JD0G mutant HSV-1 virus is deleted for ICP0 and the joint repeat elements, as described elsewhere (Reinhart et al., submitted). JD0G virus stocks were prepared and titered on U2OS cells.

Plasmid construction and transfection

A human MMP-9 cDNA clone in pCMV6-XL4 was purchased from OriGene Technologies (Rockville, MD) and cloned into pIRES1neo (Clontech Laboratories, Palo Alto, CA). Stably transfected SK-N-AS/MMP9 cells were obtained by selection with G418 (Invitrogen Corp, Carlsbad, CA).

Western blotting

Cells were lysed in 1% NP40 buffer, lysates electrophoresed through 10% SDS-polyacrylamide gels, and protein blots reacted with polyclonal anti-MMP-9 antibody (1:1,000 dilution) (Abcam, Cambridge, MA) and HRP-conjugated anti-rabbit secondary antibody (Sigma, St. Louis, MO). Blots were developed with chemiluminescence substrate (Amersham Pharmacia, Piscataway, NJ). The lower portion of each blot was reacted with polyclonal anti-β-actin antibody (Santa Cruz Biotechnology, CA) to detect loading differences.

Gelatin zymography

Conditioned media were separated on a 10% SDS-polyacrylamide gel containing 1mg/mL gelatin. The gel was washed in 10mM Tris (pH 7.5), 2.5% Triton X-100, incubated at 37°C for 16h in 50mM Tris (pH 7.5), 5mM $CaCl_2$, 1μM $ZnCl_2$, stained with Coomassie brilliant blue R-250, and destained.

Invasion assays

5×10^4 cells per well were plated in Matrigel-coated or uncoated Biocoat Invasion Chambers (BD Biosciences, San Jose, CA). At 22h, cells attached to the lower surface of the membrane were stained and counted.

Spheroid culture and imaging

Spheroids were grown to ca. 1 mm in diameter in 0.5% soft agar and individually infected in microfuge tubes with 5×10^4 pfu of JD0G virus for 2h. At 24hpi, the spheroids were fixed in 4% paraformaldehyde and 3μ Z section images of GFP expression were obtained by two-photon microscopy (Leica Microsystems Inc., Bannockburn, IL). MetaMorph software (Molecular Devices, Downingtown, PA) was used for 3-D image reconstitution analysis.

Separately, infected spheroids were trypsinized and GFP expressing cells counted under a fluorescence microscope.

Animals and tumor model

4-5-week-old female BALB/c nude mice (Charles River Laboratories, Wilmington, MA) were anesthetized and stereotactically injected with 5×10^5 SK-N-AS/MMP9 or control cells into the right frontal lobe as described (4). Animals were observed daily until death or stereotactically injected at the same coordinates with viral vector (500 pfu/2μl of JD0G) after 3 weeks. Animals were sacrificed 2 days later for analysis of the distribution of virus-infected cells in the tumor mass (IACUC protocol # 07-11-383).

Histology and immunostaining

Brain tissues were fixed in 4% paraformaldehyde for 24h and incubated in 30% sucrose for 48h. Tissues were frozen in 2-methylbutane/dry ice, embedded in OCT, sectioned at 6μm thickness, and imaged for GFP expression under an Olympus Provis fluorescence microscope (Olympus, Center Valley, PA). Alternate sections were stained with Hoechst to visualize tumor boundaries. Selected GFP-imaged sections were stained with anti-HSV antibodies (GeneTex, Irvine, CA) and Cy3-conjugated sheep anti-rabbit IgG (Sigma).

Results and Discussion

MMP-9 expression varies in brain tumor cell lines

A matching pair of high and low MMP-9-expressing brain tumor cell lines was used to examine the effects of MMP-9 activity on oHSV distribution following initial vector inoculation. Western blot analysis of cell lysates of several glioma and neuroblastoma cell lines found previously to support lytic replication of HSV identified SK-N-AS neuroblastoma and U373 glioma cells as low MMP9 expressers (Fig. 1A). Both lines were stably transfected with an MMP-9 expression plasmid. MMP-9 over-expression in the transfected pools versus the parent lines was most pronounced in SK-N-AS cells and these were used for further study (Fig. 1B).

SK-N-AS/MMP9 cells produce increased gelatinase activity, but proliferation and HSV permissiveness are unchanged

As a measure of functional activity, MMP-9 gelatinase activity was compared between SK-N-AS/MMP9 and parental cells. Gelatin zymography showed greater gelatinase activity in media from the transfected cells than the control cells (Fig. 1C). No significant difference in proliferation rate was observed between the MMP9-transfected pools and the control cells over a period of three days (Fig. 1D). To determine whether increased MMP-9 expression affected HSV infection and/or replication, SK-N-AS/MMP9 and SK-N-AS cells were infected with serial dilutions of a recently described oncolytic vector, JD0G (Reinhart et al., submitted). Plaque titers and morphology were similar on MMP-9 and control cells (not shown), indicating that increased MMP-9 expression did not alter virus entry or replication.

MMP-9 expression reduces the invasive capacity of SK-N-AS cells in vitro

ECM components are involved in intercellular communications that contribute to cell migration during embryonic development, tissue repair in adult animals (5), and tumor cell infiltration (6). Because MMP-9 is known to degrade type IV collagen, a major component of the tumor ECM, we compared the migration of SK-N-AS/MMP9 and parental cells in Matrigel-coated transwell chambers. Remarkably, SK-N-AS/MMP9 cells showed a reduced ability to migrate to the lower chamber compared to untransfected SK-N-AS cells (Fig. 2A). Quantitative analysis of the results showed an approximate difference of 2 fold (Fig. 2B;

P=0.01, Student's t-test). This observation indicated that increased MMP-9 expression on SK-N-AS cells reduced cell migration in vitro, consistent with reports showing that MMP-9 expression protects against aggressive tumor growth (7).

MMP-9 increases HSV infectivity in spheroid culture

To assess the effect of increased cellular expression of MMP-9 on HSV spread in tumor-cell spheroids, SK-N-AS/MMP9 and SK-N-AS cells were grown in soft agar to develop macroscopically visible foci and infected with JD0G virus. At 24 hpi, SK-N-AS/MMP9 spheroids showed enhanced distribution of vector-expressed GFP compared to similarly sized control SK-N-AS spheroids (Fig. 2C, upper panels). Quantification of GFP positive cells in each spheroid demonstrated an increase of approximately 3-fold in the number of transduced SK-N-AS/MMP9 over SK-N-AS cells (Fig. 2D; P=0.0019). GFP expression throughout the spheroids was imaged using a two-photon microscope. Projection of 3-micron Z sections showed enhanced infection throughout the cell mass of SK-N-AS/MMP9 spheroids compared to SK-N-AS spheroids (Fig. 2C, lower panels).

MMP-9 expression did not increase the rate of tumor progression

The contribution of MMPs to tumor growth and progression is incompletely understood, but evidence suggests that MMPs can both prevent cancer progression and encourage invasion and metastasis (7). Accordingly, we examined the growth of SK-N-AS/MMP9 and control tumors in nude mouse brains and determined whether MMP-9 contributed to the timing of tumor-induced lethality. The two lines behaved very similarly in survival experiments (Fig. 3; P=0.12) and no differences in post-mortem tumor sizes or distribution were observed (not shown).

MMP-9 enhances vector distribution following tumor injection in vivo

The finding that MMP-9 expression resulted in increased infection of tumor spheroids prompted studies to determine whether metalloproteinase expression similarly increased vector distribution following intratumoral injection in a mouse model of human brain cancer. The results of GFP imaging and anti-HSV immunostaining showed that inoculation of only 500 pfu of JD0G vector into tumors established for 21 days resulted in vector distribution throughout the tumor mass (Fig. 4C, D). Control SK-N-AS tumors showed substantially less virus infection (Fig. 4A, B).

This study was designed to test the hypothesis that MMP9 modification of the ECM produced by brain tumor cells will enhance oHSV distribution and spread. SK-N-AS has low MMP-9 activity and high susceptibility to HSV infection. We created SK-N-AS cells that constitutively express exogenous MMP-9 and found that these cells had a reduced ability to migrate in vitro. Our findings are consistent with the observation that increased MMP9 activity in vivo is associated with decreased tumor growth rate (8)and that a substantial down-regulation of MMP-9 is accompanied by a 3-fold increase in intravasation and metastasis (9). Moreover, MMP-9 antagonists at best provided no survival benefit to glioma patients (10). In contrast to these findings, it has been reported that stable transfection of the human glioblastoma cell line SNB19 with a plasmid containing antisense MMP-9 cDNA decreased the invasive properties of these cells, both in vitro and in vivo (11, 12). This discrepancy may relate to the use of different cell lines, indicating a need for direct comparisons of multiple lines to distinguish general and cell-specific effects. We will address this issue in future studies using oHSV vectors engineered to express MMP-9.

Our results comparing virus infection of both tumor spheres in vitro and brain tumors in animals showed that SK-N-AS/MMP9 cells were more susceptible to virus infection than the control SK-N-AS cells and that the infection was more widespread. MMP-9 did not

affect either infection of freshly plated cells in monolayer or tumor growth. Previous studies using Mu89 melanoma cells in a mouse skin window model showed that the treatment of tumor tissue with collagenase in combination with the oncolytic vector MGH2 resulted in enhanced vector distribution and destruction of the tumor mass without an increase in tumor spread (2). Similarly, others have observed enhanced HSV vector distribution and tumor killing using soft tissue sarcoma-derived HSTS26T cells and MMP-1 and MMP-8 to digest fibrillar collagen (3). In another study, adenovector distribution was also enhanced by MMP-8 digestion (13). Thus the principle of increasing virus spread by degradation of the ECM appears to be effective for diverse OVs and across tumor types.

While our findings indicate that modification of the ECM will facilitate homogenous vector distribution within a brain tumor mass, the exact nature of the ECM has not yet been defined for all brain tumors. Gliomas contain different collagens (14) and express multiple MMPs, including MMP-1 and MMP-3 (11, 15, 16). MMP-3 degrades proteoglycans, laminin, fibronectin and non-fibrillar collagen types, while MMP-1 degrades fibrillar collagen. In addition, these tumors express vitronectin that can be degraded by MMP-14, ADAMTS-4 and ADAMTS-5 (17, 18). Future experiments will explore the ability of MMP-9 and other MMPs to enhance oHSV vector spread and glioma tumor killing when provided as soluble proteins during vector inoculation or expressed from the vector.

Acknowledgments

References

1. Markert JM, Liechty PG, Wang W, et al. Phase Ib trial of mutant herpes simplex virus G207 inoculated pre-and post-tumor resection for recurrent GBM. Mol Ther. 2009; 17:199–207. [PubMed: 18957964]

2. McKee TD, Grandi P, Mok W, et al. Degradation of fibrillar collagen in a human melanoma xenograft improves the efficacy of an oncolytic herpes simplex virus vector. Cancer Res. 2006; 66:2509–13. [PubMed: 16510565]

3. Mok W, Boucher Y, Jain RK. Matrix metalloproteinases-1 and -8 improve the distribution and efficacy of an oncolytic virus. Cancer Res. 2007; 67:10664–8. [PubMed: 18006807]

4. Niranjan A, Moriuchi S, Lunsford LD, et al. Effective treatment of experimental glioblastoma by HSV vector-mediated TNF alpha and HSV-tk gene transfer in combination with radiosurgery and ganciclovir administration. Mol Ther. 2000; 2:114–20. [PubMed: 10947938]

5. Zamir EA, Rongish BJ, Little CD. The ECM moves during primitive streak formation--computation of ECM versus cellular motion. PLoS Biol. 2008; 6:e247. [PubMed: 18922043]

6. Martin MD, Matrisian LM. The other side of MMPs: protective roles in tumor progression. Cancer Metastasis Rev. 2007; 26:717–24. [PubMed: 17717634]

7. Coussens LM, Tinkle CL, Hanahan D, Werb Z. MMP-9 supplied by bone marrow-derived cells contributes to skin carcinogenesis. Cell. 2000; 103:481–90. [PubMed: 11081634]

8. Bendrik C, Robertson J, Gauldie J, Dabrosin C. Gene transfer of matrix metalloproteinase-9 induces tumor regression of breast cancer in vivo. Cancer Res. 2008; 68:3405–12. [PubMed: 18451168]

9. Deryugina EI, Zijlstra A, Partridge JJ, et al. Unexpected effect of matrix metalloproteinase down-regulation on vascular intravasation and metastasis of human fibrosarcoma cells selected in vivo for high rates of dissemination. Cancer Res. 2005; 65:10959–69. [PubMed: 16322244]

10. Coussens LM, Fingleton B, Matrisian LM. Matrix metalloproteinase inhibitors and cancer: trials and tribulations. Science. 2002; 295:2387–92. [PubMed: 11923519]

11. Kondraganti S, Mohanam S, Chintala SK, et al. Selective suppression of matrix metalloproteinase-9 in human glioblastoma cells by antisense gene transfer impairs glioblastoma cell invasion. Cancer Res. 2000; 60:6851–5. [PubMed: 11156378]

12. Lakka SS, Rajan M, Gondi C, et al. Adenovirus-mediated expression of antisense MMP-9 in glioma cells inhibits tumor growth and invasion. Oncogene. 2002; 21:8011–9. [PubMed: 12439751]

13. Cheng J, Sauthoff H, Huang Y, et al. Human matrix metalloproteinase-8 gene delivery increases the oncolytic activity of a replicating adenovirus. Mol Ther. 2007; 15:1982–90. [PubMed: 17653103]

14. Kunapuli P, Kasyapa CS, Hawthorn L, Cowell JK. LGI1, a putative tumor metastasis suppressor gene, controls in vitro invasiveness and expression of matrix metalloproteinases in glioma cells through the ERK1/2 pathway. J Biol Chem. 2004; 279:23151–7. [PubMed: 15047712]

15. Yoshizaki T, Sato H, Furukawa M, Pagano JS. The expression of matrix metalloproteinase 9 is enhanced by Epstein-Barr virus latent membrane protein 1. Proc Natl Acad Sci U S A. 1998; 95:3621–6. [PubMed: 9520415]

16. Choe G, Park JK, Jouben-Steele L, et al. Active matrix metalloproteinase 9 expression is associated with primary glioblastoma subtype. Clin Cancer Res. 2002; 8:2894–901. [PubMed: 12231534]

17. Chakraborti S, Mandal M, Das S, Mandal A, Chakraborti T. Regulation of matrix metalloproteinases: an overview. Mol Cell Biochem. 2003; 253:269–85. [PubMed: 14619979]

18. Chintala SK, Rao JK. Invasion of human glioma: role of extracellular matrix proteins. Front Biosci. 1996; 1:d324–39. [PubMed: 9159237]
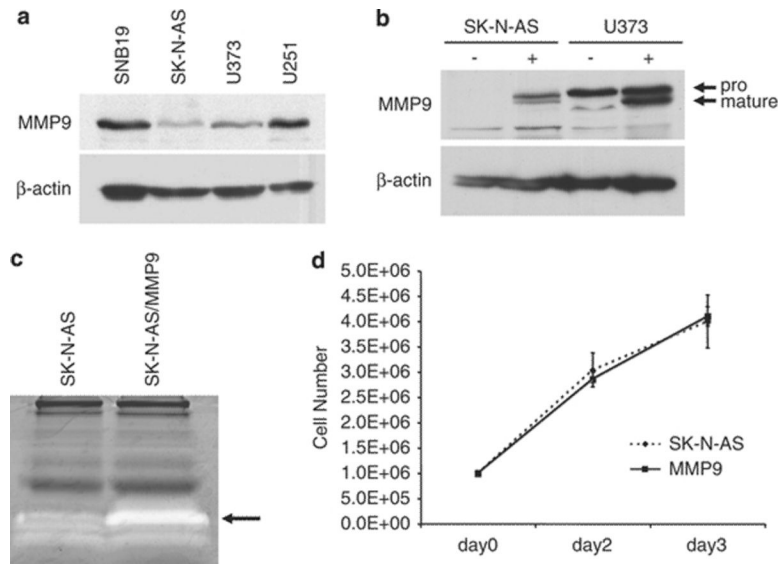
Figure 1. MMP-9 expression in brain tumor cell lines
A. Western blot analysis of MMP-9 expression in brain tumor cell lines. β-actin was visualized as a loading control. *B*. MMP-9 levels in untransfected (−) and transfected (+) SK-N-AS and U373 cells. Arrows point to the pro (92 kD) and mature (88 kD) forms of MMP-9. *C*. Gelatin zymography of conditioned medium from untransfected and MMP-9 transfected SK-N-AS cells. White bands are indicative of gelatinase activity (arrow). *D*. Growth curves of untransfected and MMP-9 transfected SK-N-AS cells in culture. Equal numbers of cells were seeded, grown for 48 or 72h, and counted. Mean values of triplicates +/− SD.
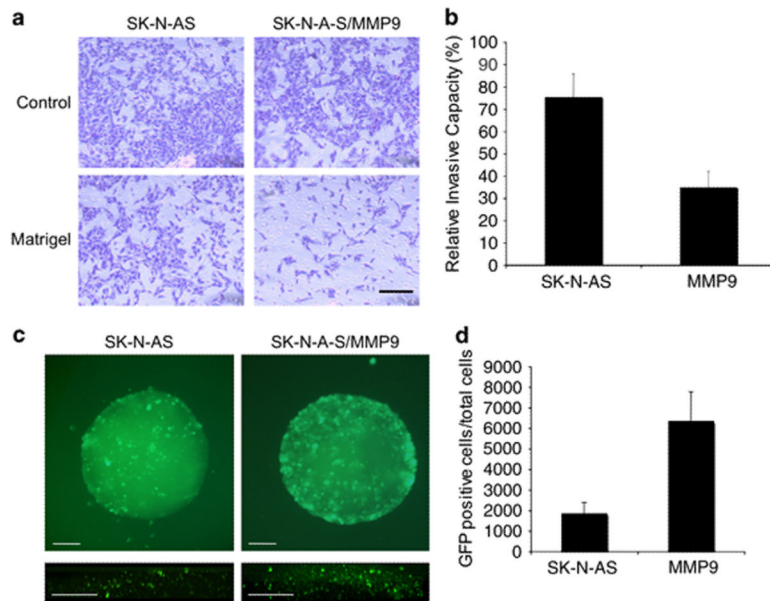
Figure 2. In vitro analysis of SK-N-AS/MMP9 cells
Untransfected and MMP-9 transfected SK-N-AS cells were plated in Matrigel-coated or uncoated (control) transwell chambers in triplicate. After 22h, cells were scraped from the upper surface of the membrane and cells attached to the lower surface were photographed (*A*) and counted (*B*). *C*. SK-N-AS and SK-N-AS/MMP9 spheroid cultures were infected with 5×10^4 pfu of JD0G virus and GFP fluorescence visualized at 24hpi in whole-mount spheroids (top) or by two-photon microscopy of fixed spheroids (bottom). Scale bars, 200μm. *D*. Individual spheroids (n=5) were trypsinized and GFP-positive cells counted under a fluorescent microscope.
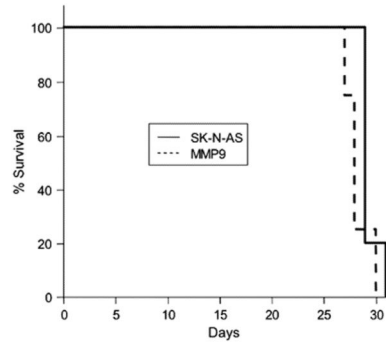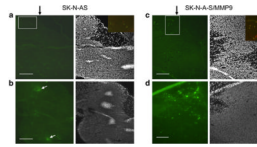
Figure 3. Survival of tumor-bearing animals
Kaplan-Meier survival plot of nude mice implanted intracerebrally with 5×10^5 SK-N-AS (n=5) or SK-N-AS/MMP9 (n=4) cells.

Figure 4. Virus infection of brain tumors
500 pfu of JD0G virus were inoculated into SK-N-AS (n=3) (*A*, *B*) and SK-N-AS/MMP9 (n=3) (*C*, *D*) brain tumors (data from four animals). Animals were sacrificed 2 days later and brain sections stained with Hoechst (grey panels) and imaged for GFP expression (green panels). Black arrows indicate the site of virus injection, white arrows point to examples of section artifacts creating false GFP signals. White boxes indicate the approximate areas of merged images of GFP fluorescence (green) and anti-HSV immunostaining (red) shown as *insets*. Scale bars, 100µm.